11-2014

Vapor-Phase Oxidation of Benzyl Alcohol Using Manganese Oxide Octahedral Molecular Sieves (OMS-2)

Naftali N. Opembe
University of Connecticut - Storrs

Curtis Guild
University of Connecticut - Storrs

Cecil King'ondu
University of Connecticut - Storrs

Nicholas C. Nelson
Iowa State University, nelsonnc@iastate.edu

Igor I. Slowing
Iowa State University, islowing@iastate.edu

Vapor-Phase Oxidation of Benzyl Alcohol Using Manganese Oxide Octahedral Molecular Sieves (OMS-2)

Abstract
Vapor-phase selective oxidation of benzyl alcohol has been accomplished using cryptomelane-type manganese oxide octahedral molecular sieve (OMS-2) catalysts. A conversion of 92% and a selectivity to benzaldehyde of 99% were achieved using OMS-2. The role played by the oxidant in this system was probed by studying the reaction in the absence of oxidant. The natures of framework transformations occurring during the oxidation reaction were fully studied using temperature-programmed techniques, as well as in situ X-ray diffraction under different atmospheres.

Disciplines
Chemistry

Comments
Reprinted (adapted) with permission from *Industrial & Engineering Chemistry Research* 53 (2014): 19044, doi:10.1021/ie5024639.

Authors
Naftali N. Opembe, Curtis Guild, Cecil King'ondu, Nicholas C. Nelson, Igor I. Slowing, and Steven L. Suib

I&EC research
Industrial & Engineering Chemistry Research

Article

pubs.acs.org/IECR

Vapor-Phase Oxidation of Benzyl Alcohol Using Manganese Oxide Octahedral Molecular Sieves (OMS-2)

Naftali N. Opembe,*[,†,‡,§] Curtis Guild,[†] Cecil King'ondu,[†,∥] Nicholas C. Nelson,[‡,§] Igor I. Slowing,[‡,§] and Steven L. Suib*[,†,‡]

[†]Department of Chemistry, University of Connecticut, 55 North Eagleville Road, Storrs, 06269-3060, United States

[‡]U.S. Department of Energy, Ames Laboratory, Ames, Iowa 50011-3020, United States

[§]Department of Chemistry, Iowa State University, Ames, Iowa 50011-3111, United States

[∥]School of Pure and Applied Science, Department of Physical Science, South Eastern Kenya University, P.O. Box 170-90200, Kitui 90200, Kenya

Supporting Information

ABSTRACT: Vapor-phase selective oxidation of benzyl alcohol has been accomplished using cryptomelane-type manganese oxide octahedral molecular sieve (OMS-2) catalysts. A conversion of 92% and a selectivity to benzaldehyde of 99% were achieved using OMS-2. The role played by the oxidant in this system was probed by studying the reaction in the absence of oxidant. The natures of framework transformations occurring during the oxidation reaction were fully studied using temperature-programmed techniques, as well as in situ X-ray diffraction under different atmospheres.

1. INTRODUCTION

Selective oxidation is a fundamentally important topic in research owing to the importance of oxidation as a unit operation in the manufacture of chemicals and chemical intermediates.[1] The products of the alcohol oxidation process, such as aldehydes, are valuable both as intermediates to other compounds and also as end products in the chemical and perfumery industries.[2] Selective oxidation of benzyl alcohol serves as a fundamental reaction for both laboratory and commercial processes.[3] An understanding of this process enables the development of oxidation processes for other organic compounds. Benzaldehyde is currently produced through the oxidation of benzyl alcohol using stoichiometric amounts of commercial manganese oxide (pyrolusite) or chromium salts in the laboratory and commercially through the chlorination and subsequent oxidation of toluene.[4] Disadvantages caused by using stoichiometric reagents and toxic salts have necessitated research into alternative pathways. Both liquid- and vapor-phase processes are possible. The vapor phase is advantageous because of the lack of downstream operations that are required in liquid-phase processes, such as solvent separation and recovery.

Laboratory-scale vapor-phase oxidation of benzyl alcohol has been accomplished using various catalysts. Table 1 presents a nonexhaustive overview of reported results and the temperatures used to achieve these results. The overview shows that both noble and non-noble metals catalyze the oxidation of benzyl alcohol in the vapor phase. This can be achieved at temperatures ranging approximately from benzyl alcohol's boiling point (205 °C) to higher temperatures (as high as 400 °C) with good selectivity.

In situ X-ray diffraction (XRD) is a powerful tool used for transformation studies of heterogeneous catalysts (oxides, carbides, sulfides, silicates, and phosphates, among others) at various intervals during the progress of a reaction. In situ XRD can identify active phases and show their stability and can also help elucidate reaction mechanisms when coupled with spectroscopic techniques such as Raman spectroscopy, Fourier transform infrared (FTIR) spectroscopy, extended X-ray absorption fine structure (EXAFS) spectroscopy, and X-ray photoelectron spectroscopy (XPS). Under reaction conditions, catalysts can undergo transformations that significantly affect their crystal structure or lattice facets. If these changes are "visualized" in situ, the results can provide a wealth of information to help improve catalyst performance or design better catalysts. In situ XRD has been utilized to study transformations of Co−Fe supported on $CaCO_3$ to show that the support reacts with the deposited metals in different

Table 1. Summary of Selected Published Benzyl Alcohol Vapor-Phase Oxidation Reactions

catalyst type	yield (%)	temperature (°C)	ref
Ag-HMS	96	310	5
nano-Au	61	240	6
K-Cu-TiO_2	99	203	7
Ag/Ni-fiber	84	380	8
Ca−Ag/SiO_2	67	240	9
Co/NaY	45	350	10
Ag/SiO_2	84	350	11
Au/TiO_2	80	320	12
Cu−Na-ZSM-5	80	400	13
1% Au−Cu/SiO_2	98	260	14

Received: June 18, 2014
Revised: November 13, 2014
Accepted: November 17, 2014
Published: November 17, 2014

dx.doi.org/10.1021/ie5024639 | Ind. Eng. Chem. Res. 2014, 53, 19044−19051

temperature regimes.[15] The complex structural transformations in $Li_{0.5}Ni_{0.25}TiOPO_4$ during electrochemical lithiation were studied using in situ XRD,[16] as was the chemical delithiation of $LiFePO_4$.[17] In situ XRD was also used to study the reduction of PdO and oxidation of Pd^0,[18] as well as the isothermal conversion of α-PcCu to β-PcCu.[19]

Cryptomelane-type octahedral molecular sieves, denoted as K-OMS-2, are a type of manganese oxide material with a tunnel structure. These materials have been prepared by different synthetic routes and extensively studied and characterized. K-OMS-2 is made up of corner- and edge-sharing manganese oxide octahedral units (MnO_6), resulting in the formation of tunnels that are partially occupied by K^+ ions and water molecules (Figure 1). The K^+ ions play the role of balancing the charge in the structure.

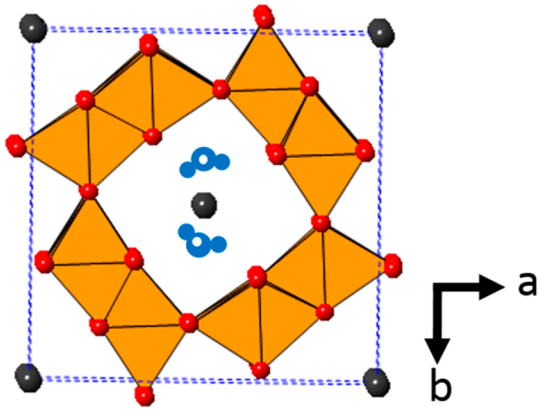

Figure 1. Crystal structure of cryptomelane-type K-OMS-2 materials with the tetragonal unit cell ($a = b = 9.886$ Å, $c = 2.8538$ Å) outlined. Black spheres represent K^+, whereas blue spheres represent water. The orange tetrahedron is composed of Mn atoms at the center and oxygen atoms at the vertices.

K-OMS-2 was thoroughly investigated in the liquid-phase oxidation of benzyl alcohol.[20] Reaction conditions for a typical batch liquid reaction were optimized at a catalyst loading of 6.25 mol %, a solvent content of 10 mL of toluene, air as the oxidant, and a reaction time of 4 h.[20]

The exemplary performance of K-OMS-2 in benzyl alcohol oxidation and its attractiveness as a less expensive alternative has led to numerous other catalytic reactions,[21−29] all performed in the liquid phase. Reported gas-phase reactions with K-OMS-2 materials have largely been confined to the total oxidation of volatile organic compounds (VOCs)[30−32] and other equally toxic compounds such as carbon monoxide (CO).[31,33−35]

Herein, we have developed a vapor-phase process for the partial oxidation of benzyl alcohol under flow conditions. The process uses K-OMS-2 as the catalyst and an oxidant gas of either 100% air or oxygen mixed in nitrogen. The benzyl alcohol is first vaporized in a heated chamber, from which its vapors meet with a stream of oxidant gas (air or pure oxygen mixed with nitrogen) and are passed through the catalyst bed. Products are collected and analyzed downstream. Importantly, close attention was paid to the transformation of the catalyst during the reaction, which was studied further using the in situ XRD and temperature-programmed reduction (TPR) and oxidation (TPO) techniques.

2. EXPERIMENTAL SECTION

2.1. Materials. Potassium permanganate ($KMnO_4$), manganese sulfate monohydrate ($MnSO_4{\cdot}H_2O$), and benzyl alcohol (99.99%, anhydrous) were purchased from Sigma-Aldrich, and concentrated nitric acid (HNO_3) was obtained from Alfa Aesar. All reagents were used without any further purification.

2.2. Catalyst Synthesis. K-OMS-2 was synthesized using an adaptation of a previously reported method.[36] In a typical reaction, 6.65 g (42 mmol) of $KMnO_4$ was added to 100 mL of distilled deionized water (DDW) to make mixture A. In another flask, 9.9 g (59 mmol) of $MnSO_4{\cdot}H_2O$ was added to 33 mL of DDW to make mixture B. Mixtures A and B were stirred separately until complete dissolution of the reagents. Then, 3.4 mL of concentrated HNO_3 was added to mixture B and further stirred. Mixture A was added dropwise to mixture B under vigorous stirring. The resultant mixture was refluxed for 24 h in an oil bath maintained at 110 °C. The product was thereafter filtered, washed until neutral to litmus test, air-dried at 120 °C for 12 h, and ground to a fine powder.

2.3. Ion Exchange. To form protonated H−K-OMS-2, 5 g of the K-OMS-2 powder was ion-exchanged (K^+ for H^+) by being dispersed in 100 mL of 1 M HNO_3, stirred at 70 °C for 6 h, and then subjected to a washing and drying procedure similar to that described in the preceding section.

2.4. Vapor-Phase Oxidation of Benzyl Alcohol. Ultra-high-purity- (UHP-) grade oxygen mixed with UHP-grade nitrogen and zero-grade air were employed as oxidants. The oxidation reactions were performed using a conventional tubular furnace that contained a vertical fixed-bed glass reactor ($h = 0.45$ m, i.d. = 9 mm), fitted with quartz wool to support 0.1−0.5 g of catalyst. Before being used in the oxidation reaction, the catalyst materials were pretreated at 120 °C overnight in an oven under air, and just before each reaction, the packed catalyst bed was further heated at the reaction temperature (210−240 °C) in pure oxygen for about 1 h. The reaction was initiated by charging benzyl alcohol into a preheated zone (220 °C), where vaporization occurred, and then mixing the vapor with a stream of oxidant and carrier gas (mixture) that was transported further into the catalyst bed. The charging rate of benzyl alcohol was varied between 0.02 and 0.5 mL/min, and that of the oxidant/carrier gas was varied between 40 and 80 sccm (standard cubic centimeters per minute). A syringe pump controlled the benzyl alcohol flow rate, and a mass flow meter controlled the oxidant/carrier gas flow rate. Liquid products and unreacted benzyl alcohol were collected using a cold trap (using solid carbon dioxide). The products were continuously collected until the entire 10 mL syringe was finished and quantitatively analyzed by gas chromatography/mass spectrometry (GC/MS). Prior to analysis, the product was vacuum-separated from water and diluted in acetone. The noncondensable gas stream was fed to an online SRI Instruments multicomponent analyzer gas chromatograph equipped with both a thermal conductivity detector (TCD) and a molecular sieve type 13X column for analysis of gaseous products.

3. CHARACTERIZATION

3.1. Crystal Structure. The crystal structure of the synthesized materials was confirmed using powder X-ray diffraction (XRD). XRD studies were performed on a Scintag XDS-2000 diffractometer using Cu Kα ($\lambda = 0.15406$ nm) radiation and operating at a beam voltage of 45 kV and a

dx.doi.org/10.1021/ie5024639 | Ind. Eng. Chem. Res. 2014, 53, 19044−19051

current of 40 mA. Diffraction data were collected continuously in the 2θ range of 5−75° at a scan rate of 1.0°/min, and phase identification was done using Joint Committee on Powder Diffraction Standards (JCPDS) file no. 29-1020. The XRD patterns of samples were collected using a glass sample holder. In situ XRD studies were performed using Cu Kα (λ = 0.15406 nm) radiation on a Thermo ARL X'tra diffractometer equipped with a Paar XRK-900 in situ reactor stage. A 2θ range of 5−75° was used with a continuous scan rate of 2.0°/min, and the phases were identified using the JCPDS database. A beam voltage and beam current of 40 kV and 44 mA, respectively, were used on a Thales MC-61 XRD tube (long fine focus). Samples were brought to the appropriate temperature under the desired atmosphere (5% H_2 in N_2 or 5% O_2 in N_2 flowing at 10 sccm) and held for 30 min prior to acquisition of the diffraction pattern.

3.2. Physical Characteristics. *3.2.1. Microscopy Studies.* Transmission electron microscopy (TEM) was carried out with a Tecnai G2 F20 electron microscope operated at 200 kV. The samples were prepared by dispersing less than 2 mg of powder in methanol and sonicating for 15 min. A drop of the dispersion was placed onto a lacey-carbon-coated copper grid and allowed to dry in air.

3.2.2. Physisorption Studies. Surface area and porosimetry analyses were performed on a Micrometrics Tristar 3000 surface area and porosity analyzer at liquid nitrogen temperature. Prior to these measurements, samples were first degassed at 100 °C for at least 6 h under a stream of nitrogen gas flowing at 100 sccm.

3.2.3. Chemisorption Studies. Chemisorption experiments were performed on a Micrometrics Autochem II 2920 instrument. Temperature-programmed desorption (TPD) experiments were performed by heating a weighed amount of the catalyst material from ambient conditions to 800 °C under a stream of helium at a rate of 10 sccm. TPR/TPO experiments were performed by heating the materials under a mixture of 10% hydrogen in He to 800 °C, cooling under He (10 sccm) back to ambient conditions, and then reheating the same material under 10% oxygen in He to 800 °C.

3.2.4. Acid Sites. Measurements of acid sites (Lewis and Brönsted) were performed by ammonia desorption. NH_3 TPD experiments were performed by first pretreating the catalyst at 120 °C under a stream of He gas, cooling back to 30 °C, adsorbing gaseous ammonia for 30 min, and then flowing He for 1 h to drive off any physisorbed ammonia from the material and the analysis lines. Temperature was then ramped at 10 °C/min to 550 °C, and the TCD signal was recorded once a stable baseline was established.

4. RESULTS

4.1. Physical, Structural and Morphological Properties. The synthesis of K-OMS-2 resulted in a black material that was ground to a fine powder in preparation for various analyses. Ion exchange of K-OMS-2 by acid treatment (forming H−K-OMS-2) did not change the color of the material significantly. XRD studies were performed on both K-OMS-2 and H−K-OMS-2 to determine their crystal phases. The XRD patterns are presented in panels i and ii, respectively, of Figure 2. Also included in Figure 2 are XRD patterns of K-OMS-2 after various treatments, namely, benzyl alcohol oxidation (Figure 2iii), benzyl alcohol oxidation in a stream of pure nitrogen as the carrier (Figure 2iv), TPD (Figure 2v), and TPR/TPO (Figure 2vi). Temperature-programmed XRD

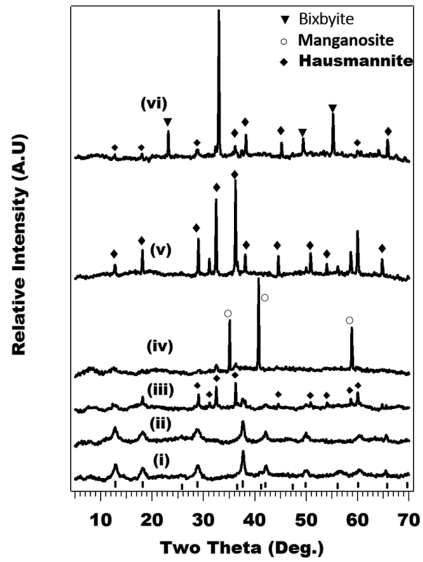

Figure 2. XRD patterns of K-OMS-2 materials: (i) K-OMS-2, (ii) H−K-OMS-2, (iii) K-OMS-2 after benzyl alcohol oxidation, (iv) K-OMS-2 after benzyl alcohol oxidation in pure N_2, (v) K-OMS-2 after TPD studies, and (vi) K-OMS-2 after TPR/TPO studies.

experiments were performed on K-OMS-2 so as to study the various transformations occurring on the catalyst during the reaction. These experiments were performed in reductive and oxidative atmospheres. TP-XRD under a stream of 5% H_2 in N_2 was performed to study the evolution of the hausmannite phase observed when benzyl alcohol was oxidized on K-OMS-2. The postreaction catalyst exhibited the presence of hausmannite, which is a more reduced form of manganese oxide than K-OMS-2. The oxidation transformation was probed by switching from H_2/N_2 gas to 5% O_2 in N_2 and heating under this atmosphere. The results of these studies are presented in Figure 3 (reduction atmosphere) and Figure 4 (oxidizing atmosphere).

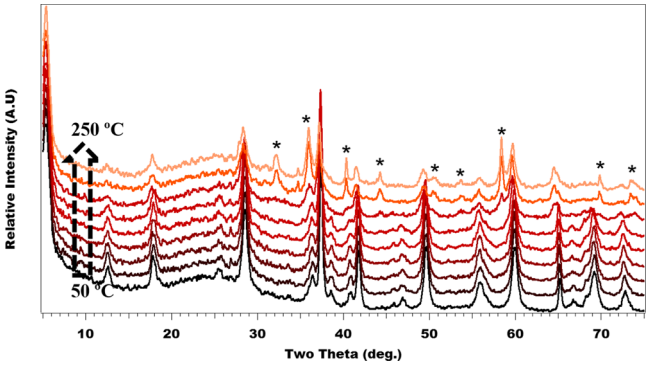

Figure 3. TP-XRD patterns of K-OMS-2 materials obtained during heating from 50 to 250 °C under 5% H_2 in N_2. The evolution of the hausmannite (Mn_3O_4) phase is shown with asterisks (*). Patterns were obtained at intervals of 25 °C.

Results of N_2 physisorption measurements at 77 K are presented in Figure 5 for both K-OMS-2 and H−K-OMS-2, and their specific surface areas and total pore volumes are reported in Table 2. These results are similar to those reported for OMS-2 materials.

High-resolution TEM micrographs of K-OMS-2 are presented in Figure 6. Figure 6A is a low-magnification micrograph of this material, whereas Figure 6B presents a high-

dx.doi.org/10.1021/ie5024639 | Ind. Eng. Chem. Res. 2014, 53, 19044−19051

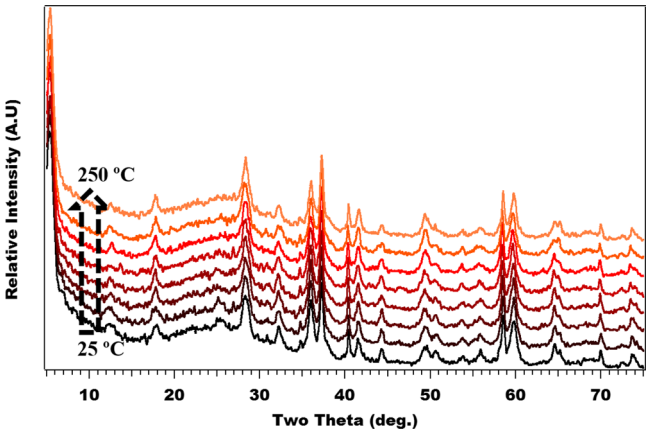

Figure 4. TP-XRD patterns of already-reduced K-OMS-2 materials obtained during heating from 25 to 250 °C under 5% O_2 in N_2. Patterns were obtained at intervals of 25 °C.

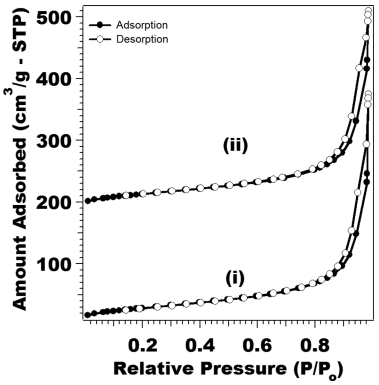

Figure 5. Nitrogen physisorption isotherms obtained for (i) K-OMS-2 and (ii) H−K-OMS-2 materials.

Table 2. Physical Properties of K-OMS-2 and H−K-OMS-2 Materials

material	SA_{BET}[a] (m^2/g)	total pore volume (cm^3/g)	total acid sites[b] (mmol/g)
K-OMS-2	102	0.359	1.59
H−K-OMS-2	103	0.357	1.83

[a]Surface area (SA) calculated using the Brunauer−Emmett−Teller (BET) method. [b]Total acid sites quantified from NH_3 TPD profiles in Figure S2 (Supporting Information).

magnification image of the same material that reveals more information.

4.2. Acidity Measurements, Chemisorption Studies, and Temperature-Programmed Techniques. TPD measurements were carried out by heating the materials in pure He to study the structural changes and evolution of oxygen from the materials with increasing temperature. These results are presented in Figure S1 (Supporting Information). The NH_3 TPD study (Figure S2 of Supporting Information) was aimed at determining the presence of acid sites on the materials. TPR/TPO was performed by heating K-OMS-2 under a stream of 10% H_2 in He (TPR) to 800 °C, allowing the ,material to cooled to ambient temperature, and then performing TPO on the same material with 10% O_2 in He. These results are shown in Figure S3 (Supporting Information).

4.3. Catalytic Results. Analysis of the liquid products collected in the cold trap revealed a good composition of the

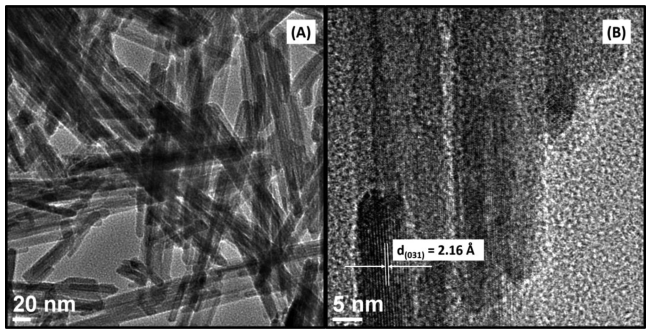

Figure 6. High-resolution TEM micrographs of K-OMS-2 taken at (A) low and (B) high magnifications.

oxidized products, as benzaldehyde was the predominant product when oxygen or air was used as the oxidant. These results are presented in Table 3. H−K-OMS-2 showed a slightly superior performance than K-OMS-2. The selectivity to benzoic acid was only about 1% with H−K-OMS-2 compared to 4% with K-OMS-2 (Table 3, entries 2 and 3, respectively). In these studies, the composition of the gas stream was 62.5% O_2 by volume. However, use of pure air (compressed) delivered at similar flow rates was studied, as was the use of pure nitrogen (absence of an oxidizing component). These results are presented in Table 3, entries 4 and 5, respectively. The difference in performance upon use of pure air was negligible (entry 4), indicating that compressed air can also be used as the oxidant in place of mixed O_2/N_2. The rate at which benzyl alcohol was delivered (at a constant carrier flow) was found to be important, as use of different benzyl alcohol flow rates led to different results. When benzyl alcohol was delivered at 0.002 mL/min, the conversion was comparable to that obtained when it was delivered at 0.02 mL/min, but the selectivity was compromised. At a benzyl alcohol flow rate of 0.002 mL/min, the amount of benzoic acid increased to 12% of the product composition compared to only 1% when the flow rate was 0.02 mL/min. When the rate was increased to 0.1 and 0.5 mL/min, the conversion dropped to 64% and 58%, respectively, but the drop in selectivity was not as pronounced (Figure 7). In either case, the product that showed an increase in selectivity was the ester. On the other hand, a change in oxidant/carrier flow rate from 40 to 80 sccm led to a drop in alcohol conversion from 92% to 81% (entry 2 vs entry 6), indicating that the flow rate of oxidant (and, hence, the residence time of the catalyst) is also a crucial factor. This increase in carrier flow rate was achieved by increasing the flow of N_2 but maintaining that of O_2 at the original set value. The progress of the reaction was also monitored by sampling at every 1 h. These results are shown in Figure 8. Rapid increases in both conversion and selectivity occurred in the first hour, and after that, small increases occurred until steady-state conditions were achieved. When the same catalyst was reused, there was no noticeable change in activity after an 8-h reaction period.

5. DISCUSSION

The wet chemical synthesis of K-OMS-2 through the precipitation route has been widely studied.[36−40] This process was reported to be favorable under acidic conditions by Portehault et al.,[41] who showed that, in a matter of minutes after mixing of the synthesis mixtures, the oxidation process proceeds to about 99%. This is a comproportionation reaction

dx.doi.org/10.1021/ie5024639 | Ind. Eng. Chem. Res. 2014, 53, 19044−19051

Table 3. Results of the Vapor-Phase Oxidation of Benzyl Alcohol Using Manganese Oxide Octahedral Molecular Sieve Catalysts[a]

				selectivity (%)			
entry	oxidant/carrier flow rate (sccm)	alcohol flow rate (mL/min)	conversion (%)	aldehyde	acid	ester	TON[b]
1	40	0.002	93	88	12	0	204
2	40	0.02	92	99	1	0	202
3[c]	40	0.02	92	96	4	0	202
4[d]	40	0.02	91	99	1	0	200
5[e]	40	0.02	95	7	93	0	–
6	80	0.02	81	93	1	6	178
7	40	0.10	64	98	1	1	140
8	40	0.50	58	93	1	6	119

[a]Conditions (unless indicated otherwise): 0.35 g (0.4375 mmol) of catalyst, 210 °C, 25 sccm O_2, and 15 sccm N_2. Unless indicated otherwise, all reactions were performed using H−K-OMS-2 catalyst. [b]Turnover number (TON) calculated based on number of moles of reactants converted divided by number of moles of catalyst. Total number of moles of benzyl alcohol fed (96 mmol) used as the standard. [c]Reaction performed using K-OMS-2. [d]Compressed air at 40 sccm used. [e]Compressed nitrogen at 40 sccm used.

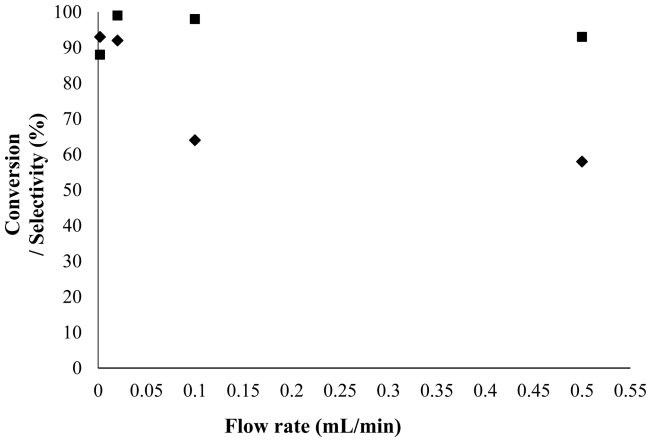

Figure 7. Conversion (♦) and selectivity (■) as functions of benzyl alcohol flow rate with a catalyst loading of 0.35 mmol.

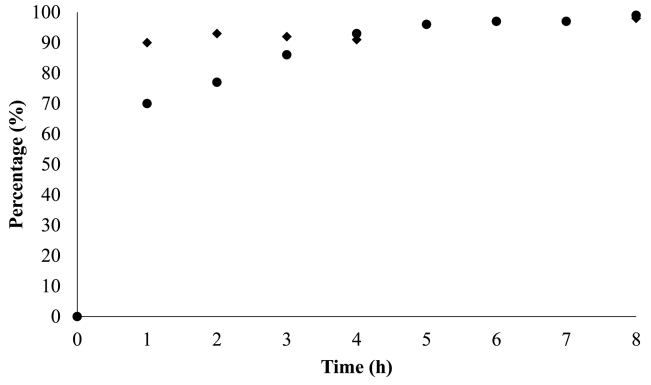

Figure 8. Conversion (●) and selectivity (♦) as functions of time with a catalyst loading at 0.35 mmol.

involving the oxidation of Mn^{2+} and the simultaneous reduction of MnO_4^-.

Liquid-phase oxidation reactions using K-OMS-2 materials have also been extensively studied and reported. Son et al.[20] pioneered the oxidation of benzyl alcohol in the liquid phase, thereby opening the possibility of application of K-OMS-2 to other organic compounds. However, partial oxidation of organic compounds in the vapor phase has not been explored, and few to no reports on this topic are available.

This report is the first attempt at the vapor-phase partial oxidation of benzyl alcohol using K-OMS-2. This reaction was achieved through systematic studies to determine the best experimental conditions for the vapor-phase reaction, considering the catalyst loading, benzyl alcohol flow rate, oxidant flow rate, and reaction temperature. This reaction was attempted at temperatures as high as 250 °C and proceeded to good yields, but 210 °C was selected as a compromise at which the yield of benzaldehyde was still high yet the temperature was just above the benzyl alcohol boiling point. Similarly, results obtained using 0.5 g of catalyst were similar to those obtained at a 0.35-g loading. Loadings of less than 0.35 g resulted in low activity.

XRD analyses of both K-OMS-2 and H−K-OMS-2 revealed similar patterns with no noticeable shifts in the peaks that can be indexed to the mineral compound cryptomelane (Q-phase) using JCPDS file no. 29-1020. Under the chosen synthesis conditions, the material crystallizes in the tetragonal phase (space group $I4/m$, lattice parameters $a = b = 9.886$ Å and $c = 2.8538$ Å). Both materials were subjected to benzyl alcohol oxidation, and their postreaction structures were analyzed again using XRD. Again, their relative patterns after reaction showed no noticeable differences but were markedly different from those of the respective starting materials. As can be seen in Figure 2iii, these patterns revealed a mixture of two phases, a cryptomelane phase with a secondary phase (labeled) that can be indexed to that of the mineral hausmannite (Mn_3O_4). In an attempt to study the contribution of oxygen (in the carrier mixture) to the stability of the cryptomelane phase during the oxidation reaction, the same reaction was performed using pure nitrogen instead of the initial mixture. The postreaction catalyst was subjected to XRD, and the resultant patterns shown in Figure 2iv reveal a predominant manganosite (MnO) phase, which is the most reduced phase of all of the manganese oxide polymorphs. In K-OMS-2, manganese exists predominantly in the oxidation state of 4+, with minor amounts of 3+ and 2+ present.[42] When K-OMS-2 was used in the benzyl alcohol oxidation reaction in the liquid phase, the postreaction XRD patterns of the catalyst showed no structural changes.[22,29] In the vapor-phase reaction, however, some of the manganese in the 4+ and 3+ states was reduced to lower oxidation states, resulting in the creation of hausmannite and manganosite in the presence and absence, respectively, of oxygen. Oxygen prevents deep reduction from occurring. Because not all of the Mn^{4+} ions are converted to Mn^{3+}/Mn^{2+} in the presence of oxygen whereas all of the Mn^{4+} ions are evidently converted to Mn^{2+} in

dx.doi.org/10.1021/ie5024639 | Ind. Eng. Chem. Res. 2014, 53, 19044−19051

the absence of oxygen, oxygen plays a role in partially reoxidizing the manganese in the lower oxidation states back to the higher states or preventing the complete reduction to Mn^{2+}. This was confirmed by carrying out the oxidation reaction in the presence of pure nitrogen, in which the postreaction phase was pure MnO meaning all of the manganese ions were reduced to the 2+ oxidation state. This reduction is only possible during benzyl alcohol oxidation or treatment of K-OMS-2 with a reducing gas at higher temperatures. In situ XRD experiments were performed on K-OMS-2 in the presence of a stream of H_2 in N_2, and the results showed the evolution of hausmannite with temperature at 250 °C. These results confirmed the observations made during benzyl alcohol oxidation. Cooling the already-reduced K-OMS-2 under N_2 to room temperature did not lead to any phase change (see Figure S4 of Supporting Information). TPD revealed ongoing structural changes as the material was heated. The lower-temperature peak (~550 °C) in the TPD scan was a result of the evolution of lattice oxygen from K-OMS-2, which resulted in the formation of Mn_2O_3. The TPD peak at higher temperature (~600−750 °C) was a result of the evolution of structural oxygen and resulted in the formation of Mn_3O_4, as can be seen in Figure S1 of the Supporting Information. An XRD pattern of this material reveals the Mn_3O_4 phase (Figure 2v). Similar transformations have been reported by DeGuzman et al.[36] The TPR/TPO results (see Figure S3 of Supporting Information) indicated a high consumption (9.76 mmol) of H_2 during reduction compared to 2.32 mmol of oxygen consumed during the reoxidation step. The XRD pattern of the reoxidized material (during TPO) revealed a mixture of bixbyite phase with hausmannite phase as the only phases present (Figure 2vi). However, prior to TPO, the furnace had to be cooled to room temperature under an inert gas, which afforded time to check the material's color. This color was green, indicating a complete reduction to MnO. This is the same color as observed during benzyl alcohol oxidation with pure nitrogen as the oxidant. The NH_3 TPD results (see Figure S2 of Supporting Information) show three desorption peaks at 65, 150, and 250 °C for both K-OMS-2 and H−K-OMS-2. This could be the result of three distinct types of acidic sites on the materials. The total acid site contents were found to be 1.59 and 1.83 mmol/g for K-OMS-2 and H−K-OMS-2, respectively.

The vapor-phase oxidation of benzyl alcohol proceeds to good conversions at various flow rates. The best conversion under oxidizing conditions was realized when the alcohol flow rate was intermediate (0.02 mL/min), leading predominantly to benzaldehyde, whereas lower rates (0.002 mL/min) led to increased production of benzoic acid. Rates higher than 0.02 mL/min led to a decrease in conversion. When performed in the absence of oxygen, the oxidation yielded predominantly benzyl benzoate. Benzyl benzoate is a product of the esterification reaction of benzaldehyde and benzyl alcohol. The presence of oxygen suppresses this reaction in favor of benzaldehyde. The effect of the formation of benzyl benzoate is a deep reduction of manganese in the catalyst (to MnO), as can be seen in Figure 2iii. The implications of these reduction processes on the catalyst is that, during reaction in the presence of oxygen, the catalyst cannot be reduced fully, as oxygen causes reoxidation back to higher oxidation states. However, complete regeneration of the partially reduced K-OMS-2 could not be achieved under the conditions of this study. Because K-OMS-2 is stabilized by the presence of both K^+ and H_2O in the tunnels, heating it under a reducing atmosphere, apart from reducing the material, also drives off this H_2O, which aids in the apparent difficulty in regenerating to K-OMS-2 in the absence of H_2O. This premise is supported by in situ XRD results that showed the emergence of hausmannite when K-OMS-2 was heated under a reducing environment at about 200−250 °C (Figure 3). This phase is stable upon cooling to room temperature (see Figure S4 of Supporting Information) and does not transform upon being heated under oxidizing conditions (Figure 4).

6. CONCLUSIONS

A vapor-phase process for the oxidation of neat benzyl alcohol to benzaldehyde using K-OMS-2 catalyst has been developed. The process utilizes atmospheric air or oxygen diluted in nitrogen as the oxidant. This process, just like its liquid-phase counterpart, leads to high turnovers (>200) and selectivities (98%). The phenomena of K-OMS-2 structural changes during the reaction were explored using conditions similar to those emplyed for the oxidation reaction but utilizing hydrogen. This was achieved using both TP-XRD and TPR/TPO techniques. These analyses conclusively revealed that benzyl alcohol oxidation on K-OMS-2 leads to changes (reductions) in the oxidation state of manganese. The extent of this reduction is dependent on the presence or lack of an oxidizing molecule. When the reaction is performed in oxygen, only partial reduction occurs, whereas complete (deep) reduction of manganese to Mn^{2+} occurs when no oxygen is employed. This means that oxygen prevents the deep reduction of manganese and also is involved in the regeneration of higher oxidation states.

■ ASSOCIATED CONTENT

Supporting Information

Additional information as noted in text. This material is available free of charge via the Internet at http://pubs.acs.org.

■ AUTHOR INFORMATION

Corresponding Authors

*E-mail: nopembe@gmail.com.
*E-mail: steven.suib@uconn.edu.

Notes

The authors declare no competing financial interest.

■ ACKNOWLEDGMENTS

N.N.O., C.G., C.K., and S.L.S. acknowledge support from the U.S. Department of Energy, Office of Basic Energy Sciences, Division of Chemical, Geological, and Biological Sciences, under Grant DE-FG02-86ER13622.A000. TEM micrographs (taken by NN), Physisorption, Chemisorption, and additional catalytic tests were performed at The Ames Laboratory. This research was supported by the U.S. Department of Energy, Office of Basic Energy Sciences (BES), Division of Chemical Sciences, Geosciences, and Biosciences through the Ames Laboratory (T.K., D.S.-A., I.I.S., M.P.). The Ames Laboratory is operated for the U.S. Department of Energy by Iowa State University under Contract No. DE-AC02−07CH11358.

■ REFERENCES

(1) DeGuzman, R. N.; Shen, Y.-N.; Neth, E. J.; Suib, S. L.; O'Young, C.-L.; Levine, S.; Newsam, J. M. Selective liquid-phase oxidation of alcohols catalyzed by a silver-based catalyst promoted by the presence of ceria. *J. Catal.* **2009**, *266*, 320.

(2) Beller, M.; Bolm, C. *Transition Metals for Organic Synthesis: Building Blocks and Fine Chemicals*; Wiley: New York, 2004.
(3) Brink, G-J. T.; Arends, I. W. C. E.; Sheldon, R. A. Green, Catalytic Oxidation of Alcohols in Water. *Science* **2000**, *287*, 1636.
(4) *Kirk-Othmer Encyclopedia of Chemical Technology*, 4th ed.; Kroschwitz, J. I., Howe-Grant, M., Eds.; Wiley: New York, 1992.
(5) Jia, L.; Zhang, S.; Gu, F.; Ping, Y.; Guo, X.; Zhong, Z.; Su, F. Highly selective gas-phase oxidation of benzyl alcohol to benzaldehyde over silver-containing hexagonal mesoporous silica. *Microporous Mesoporous Mater.* **2012**, *149*, 158.
(6) Han, D.; Xu, T.; Su, J.; Xu, J.; Ding, Y. Gas-Phase Selective Oxidation of Benzyl Alcohol to Benzaldehyde with Molecular Oxygen over Unsupported Nanoporous Gold. *ChemCatChem* **2010**, *2*, 383.
(7) Fan, J.; Dai, Y.; Li, Y.; Zheng, N.; Guo, J.; Yan, X.; Stucky, G. D. Low-Temperature, Highly Selective, Gas-Phase Oxidation of Benzyl Alcohol over Mesoporous K-Cu-TiO_2 with Stable Copper(I) Oxidation State. *J. Am. Chem. Soc.* **2009**, *131*, 15568.
(8) Mao, J.; Deng, M.; Xue, Q.; Chen, L.; Lu, Y. Thin-sheet Ag/Ni-fiber catalyst for gas-phase selective oxidation of benzyl alcohol with molecular oxygen. *Catal. Commun.* **2009**, *10*, 1376.
(9) Sawayama, Y.-S.; Shibahara, H.; Ichihashi, Y.; Nishiyama, S.; Tsuruya, S. Promoting Effect and Role of Alkaline Earth Metal Added to Supported Ag Catalysts in the Gas-Phase Catalytic Oxidation of Benzyl Alcohol. *Ind. Eng. Chem. Res.* **2006**, *45*, 8837.
(10) Nakashima, D.; Ichihashi, Y.; Nishiyama, S.; Tsuruya, S. Promoted partial oxidation activity of alkali metal added-Co catalysts supported on NaY and NaUSY zeolites in the gas-phase catalytic oxidation of benzyl alcohol. *J. Mol. Catal. A: Chem.* **2006**, *259*, 108.
(11) Yamamoto, R.; Sawayama, Y.-S.; Shibahara, H.; Ichihashi, Y.; Nishiyama, S.; Tsuruya, S. Promoted partial oxidation activity of supported Ag catalysts in the gas-phase catalytic oxidation of benzyl alcohol. *J. Catal.* **2005**, *234*, 308.
(12) Kumar, A.; Kumar, V. P.; Kumar, B. P.; Vishwanathan, V.; Chary, K. V. R. Vapor Phase Oxidation of Benzyl Alcohol Over Gold Nanoparticles Supported on Mesoporous TiO_2. *Catal. Lett.* **2014**, *144*, 1459.
(13) Hayashibara; Nishiyama, S.; Tsuruya, S.; Masai, M. The Effect of Alkali Promoters on Cu-Na-ZSM-5 Catalysts in the Oxidation of Benzyl Alcohol. *J. Catal.* **1995**, *153*, 254.
(14) Pina, C. D.; Falletta, E.; Rossi, M. Highly selective oxidation of benzyl alcohol to benzaldehyde catalyzed by bimetallic gold−copper catalyst. *J. Catal.* **2008**, *260*, 384.
(15) Chiwaye, N.; Jewell, L. L.; Billing, D. G.; Naidoo, D.; Ncube, M.; Coville, N. J. *In situ* powder XRD and Mössbauer study of Fe−Co supported on $CaCO_3$. *Mater. Res. Bull.* **2014**, *56*, 98.
(16) Eriksson, R.; Maher, K.; Saadoune, I.; Mansori, M.; Gustafsson, T.; Edström, K. Electrochemical lithium ion intercalation in $Li_{0.5}Ni_{0.25}TiOPO_4$ examined by in situ X-ray diffraction. *Solid State Ionics* **2012**, *225*, 547.
(17) Wang, X.-J.; Chen, H.-Y.; Yu, X.; Wu, L.; Nam, K.-W.; Bai, J.; Li, H.; Huang, X.; Yang, X.-Q. A new in situ synchrotron X-ray diffraction technique to study the chemical delithiation of $LiFePO_4$. *Chem. Commun.* **2011**, *47*, 7170.
(18) Baylet, A.; Marecot, P.; Duprez, D.; Castellazzi, P.; Groppi, G.; Forzatti, P. In situ Raman and in situ XRD analysis of PdO reduction and Pd° oxidation supported on γ-Al_2O_3 catalyst under different atmospheres. *Phys. Chem. Chem. Phys.* **2011**, *13*, 4607.
(19) Ballirano, P.; Caminiti, R. Kinetics of α-PcCu → β-PcCu Isothermal Conversion in Air and Thermal Behavior of β-PcCu from in Situ Real-Time Laboratory Parallel-Beam X-ray Powder Diffraction. *J. Phys. Chem. A* **2009**, *113*, 7774.
(20) Son, Y.-S.; Makwana, V. D.; Howell, A. R.; Suib, S. L. Efficient, Catalytic, Aerobic Oxidation of Alcohols with Octahedral Molecular Sieves. *Angew. Chem., Int. Ed.* **2001**, *40*, 4280.
(21) Opembe, N. N.; King'ondu, C. K.; Suib, S. L. Efficient Oxidation of 2,3,6-Trimethyl Phenol Using Non-Exchanged and H^+ Exchanged Manganese Oxide Octahedral Molecular Sieves (K-OMS-2 and H−K-OMS-2) as Catalysts. *Catal. Lett.* **2012**, *142*, 427.
(22) Opembe, N. N.; Son, Y.-S.; Sriskandakumar, T.; Suib, S. L. Kinetics and Mechanism of 9*H*-Fluorene Oxidation Catalyzed by Manganese Oxide Octahedral Molecular Sieves. *ChemSusChem* **2008**, *1*, 182.
(23) Kumar, R.; Garces, L. J.; Son, Y.-S.; Suib, S. L.; Malz, R. E. Manganese oxide octahedral molecular sieve catalysts for synthesis of 2-aminodiphenylamine. *J. Catal.* **2005**, *236*, 287.
(24) Kumar, R.; Sithambaram, S.; Suib, S. L. Cyclohexane oxidation catalyzed by manganese oxide octahedral molecular sieves—Effect of acidity of the catalyst. *J. Catal.* **2009**, *262*, 304.
(25) Ghosh, R.; Son, Y.-S.; Makwana, V. D.; Suib, S. L. Liquid-phase epoxidation of olefins by manganese oxide octahedral molecular sieves. *J. Catal.* **2004**, *224*, 288.
(26) Kona, J. R.; King'ondu, C. K.; Howell, A. R.; Suib, S. L. OMS-2 for Aerobic, Catalytic, One-Pot Alcohol Oxidation-Wittig Reactions: Efficient Access to α,β-Unsaturated Esters. *ChemCatChem* **2014**, *6*, 749.
(27) Dharmarathna, S.; King'ondu, C. K.; Pahalagedara, L.; Kuo, C.-H.; Zhang, Y.; Suib, S. L. Manganese octahedral molecular sieve (OMS-2) catalysts for selective aerobic oxidation of thiols to disulfides. *Appl. Catal. B* **2014**, *147*, 124.
(28) Sithambaram, S.; Xu, L.; Chen, C.-H.; Ding, Y.; Kumar, R.; Calvert, C.; Suib, S. L. Manganese octahedral molecular sieve catalysts for selective styrene oxide ring opening. *Catal. Today* **2009**, *140*, 162.
(29) Sithambaram, S.; Nyutu, E. K.; Suib, S. L. OMS-2 catalyzed oxidation of tetralin: A comparative study of microwave and conventional heating under open vessel conditions. *Appl. Catal. A* **2008**, *348*, 214.
(30) Genuino, C. H.; Dharmarathna, S.; Njagi, C. E.; Mei, C. M.; Suib, S. L. Gas-Phase Total Oxidation of Benzene, Toluene, Ethylbenzene, and Xylenes Using Shape-Selective Manganese Oxide and Copper Manganese Oxide Catalysts. *J. Phys. Chem. C* **2012**, *116*, 12066.
(31) Luo, J.; Zhang, Q.; Garcia-Martinez, J.; Suib, S. L. Adsorptive and Acidic Properties, Reversible Lattice Oxygen Evolution, and Catalytic Mechanism of Cryptomelane-Type Manganese Oxides as Oxidation Catalysts. *J. Am. Chem. Soc.* **2008**, *130*, 3198.
(32) Luo, J.; Zhang, Q.; Huang, A.; Suib, S. L. Total oxidation of volatile organic compounds with hydrophobic cryptomelane-type octahedral molecular sieves. *Microporous Mesoporous Mater.* **2000**, *35*−*36*, 209.
(33) Özacar, M.; Poyraz, A. S.; Genuino, C. H.; Kuo, C.-H.; Meng, Y.; Suib, S. L. Influence of silver on the catalytic properties of the cryptomelane and Ag-hollandite types manganese oxides OMS-2 in the low-temperature CO oxidation. *Appl. Catal. A* **2013**, *462*−*463*, 64.
(34) Ching, S.; Kriz, A. D.; Luthy, M. K.; Njagi, E. C.; Suib, S. L. Self-assembly of manganese oxide nanoparticles and hollow spheres. Catalytic activity in carbon monoxide oxidation. *Chem. Commun.* **2011**, *47*, 8286.
(35) Xia, G. G.; Yin, Y. G.; Willis, W. S.; Wang, J. Y.; Suib, S. L. Efficient Stable Catalysts for Low Temperature Carbon Monoxide Oxidation. *J. Catal.* **1999**, *185*, 91.
(36) DeGuzman, R. N.; Shen, Y.-F.; Neth, J. E.; Suib, S. L.; O'Young, C.-L.; Levine, A.; Newsam, J. M. Synthesis and Characterization of Octahedral Molecular Sieves (OMS-2) Having the Hollandite Structure. *Chem. Mater.* **1994**, *6*, 815−821.
(37) Yuan, J.; Li, W.-N.; Gomez, S.; Suib, S. L. Shape-Controlled Synthesis of Manganese Oxide Octahedral Molecular Sieve Three-Dimensional Nanostructures. *J. Am. Chem. Soc.* **2005**, *127*, 14184.
(38) Malinger, A. K.; Ding, Y.-S.; Sithambaram, S.; Espinal, L.; Gomez, S.; Suib, S. L. Microwave frequency effects on synthesis of cryptomelane-type manganese oxide and catalytic activity of cryptomelane precursor. *J. Catal.* **2006**, *239*, 290.
(39) Villegas, C. V.; Garces, J. L.; Gomez, S.; Durand, P. J.; Suib, S. L. Particle Size Control of Cryptomelane Nanomaterials by Use of H_2O_2 in Acidic Conditions. *Chem. Mater.* **2005**, *17*, 1910.
(40) King'ondu, C. K.; Opembe, N. N.; Chen, C.-H.; Ngala, K.; Huang, H.; Iyer, A.; Garcés, F. H.; Suib, S. L. Manganese Oxide Octahedral Molecular Sieves (OMS-2) Multiple Framework Sub-

stitutions: A New Route to OMS-2 Particle Size and Morphology Control. *Adv. Funct. Mater.* **2011**, *21*, 312.
(41) Portehault, D.; Cassaignon, S.; Baudrin, E.; Jolivet, J.-P. Morphology Control of Cryptomelane Type MnO_2 Nanowires by Soft Chemistry. Growth Mechanisms in Aqueous Medium. *Chem. Mater.* **2007**, *19*, 5410.
(42) Shen, S.-F.; Ding, Y.-S.; Liu, J.; Han, Z.-H.; Budnick, I. J.; Hines, A. W.; Suib, S. L. A Magnetic Route to Measure the Average Oxidation State of Mixed-Valent Manganese in Manganese Oxide Octahedral Molecular Sieves (OMS). *J. Am. Chem. Soc.* **2005**, *127*, 6166.